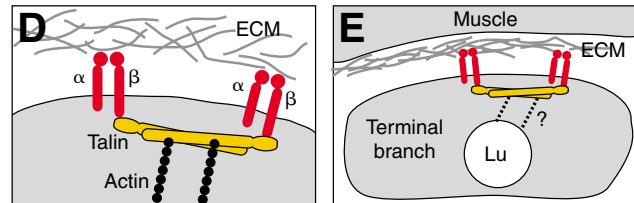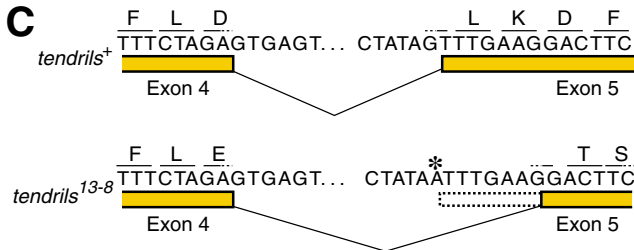## *Drosophila* talin and integrin genes are required for maintenance of tracheal terminal branches and luminal organization

Boaz P. Levi, Amin S. Ghabrial and Mark A. Krasnow *Development* **133**, 2383-2393.

One of the gene labels on chromosome 3 in Fig. 4A was misaligned. A corrected version of the figure is printed below.

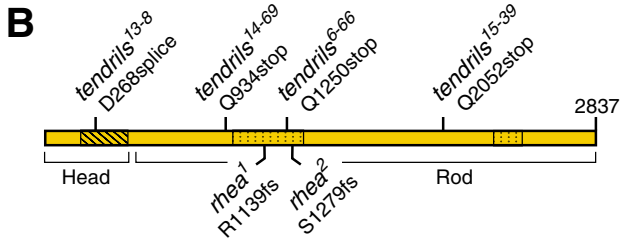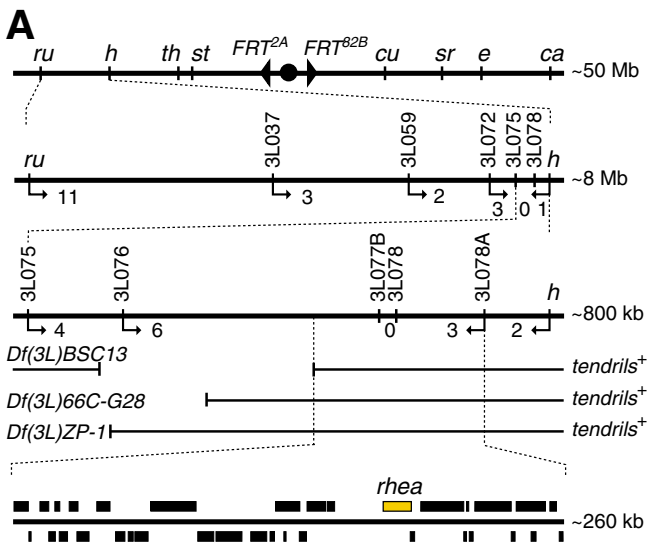We apologise to authors and readers for this mistake.

Drosophila talin and integrin genes are required for maintenance of tracheal terminal branches and luminal organization

Boaz P. Levi, Amin S. Ghabrial and Mark A. Krasnow*

Epithelial tubes that compose many organs are typically long lasting, except under specific developmental and physiological conditions when network remodeling occurs. Although there has been progress elucidating mechanisms of tube formation, little is known of the mechanisms that maintain tubes and destabilize them during network remodeling. Here, we describe *Drosophila tendrils* mutations that compromise maintenance of tracheal terminal branches, fine gauge tubes formed by tracheal terminal cells that ramify on and adhere tightly to tissues in order to supply them with oxygen. Homozygous *tendrils* terminal cell clones have fewer terminal branches than normal but individual branches contain multiple convoluted lumens. The phenotype arises late in development: terminal branches bud and form lumens normally early in development, but during larval life lumens become convoluted and mature branches degenerate. Their lumens, however, are retained in the remaining branches, resulting in the distinctive multi-lumen phenotype. Mapping and molecular studies demonstrate that *tendrils* is allelic to *rhea,* which encodes *Drosophila* talin, a large cytoskeletal protein that links integrins to the cytoskeleton. Terminal cells mutant for *myospheroid*, the major *Drosophila* β-integrin, or doubly mutant for *multiple edematous wings* and *inflated* α-integrins, also show the *tendrils* phenotype, and localization of *myospheroid* β-integrin protein is disrupted in *tendrils* mutant terminal cells. The results provide evidence that integrin-talin adhesion complexes are necessary to maintain tracheal terminal branches and luminal organization. Similar complexes may stabilize other tubular networks and may be targeted for inactivation during network remodeling events.

KEY WORDS: *Drosophila*, Talin, Trachea, Integrin, Tube morphogenesis

INTRODUCTION

Many organs are composed of networks of tubes that transport and modify gases and liquids (Hogan and Kolodziej, 2002; Lubarsky and Krasnow, 2003; O'Brien et al., 2002). The tube walls are typically an epithelial sheet of cells with the apical surface lining the lumen, in direct contact with the transported substance. During development, the cells are shaped to create tubes of different length, gauge, cellular architecture and branching pattern that are tailored to organ function. Once formed, tubes are usually maintained for long periods. However, at specific times during development or under certain physiological conditions, some tubular networks rearrange or undergo dramatic remodeling events. These include pruning or complete elimination of branches, as occurs during metamorphosis of insect tracheal (respiratory) systems (Whitten, 1957), during conversion of primitive vascular plexi into mature blood vessel networks during vertebrate development (Risau and Flamme, 1995), during mammary gland involution after weaning (Green and Lund, 2005) and following treatment of tumors with anti-angiogenesis drugs (Inai et al., 2004). Although progress has been made identifying mechanisms that control branch outgrowth and tube morphogenesis, much less is known of the molecular events that stabilize tubes and destabilize them during remodeling events. Here, we describe a gene required for maintenance of terminal branches of the *Drosophila* tracheal system.

The larval tracheal system of *Drosophila* is a network of thousands of interconnected tubes that delivers oxygen to tissues (Fig. 1A,B) (Manning and Krasnow, 1993; Rühle, 1932). Air enters the network and diffuses through primary, secondary and terminal branches to reach the tissues (Wigglesworth, 1972). Terminal branches (tracheoles) are fine gauge tubes, ranging from 0.1-1.0 μm in diameter (Fig. 1C,D) (Wigglesworth and Lee, 1982). These blind-ended tubes ramify extensively on and attach tightly to internal tissues to facilitate gas exchange (Manning and Krasnow, 1993; Noirot and Noirot-Thimotee, 1982). The attachments are generally long lived, although under certain conditions, cellular projections from oxygen-starved cells can bind to and redistribute nearby terminal branches to satisfy their oxygen need (Wigglesworth, 1959; Wigglesworth, 1977).

The tracheal system arises during mid-embryogenesis from ten pairs of epithelial sacs, each of which forms a hemi-segment of the larval tracheal network (Samakovlis et al., 1996). Small groups of tracheal cells migrate out from each sac to form primary branches, guided by *branchless* FGF (Sutherland et al., 1996). Some cells at the tips of budding primary branches form unicellular secondary branches sealed by an autocellular junction. These same cells go on to form terminal branches by extending long cellular projections towards oxygen-starved, *branchless*-expressing cells in the target tissues (Guillemin et al., 1996; Jarecki et al., 1999). A lumen then forms within each projection by a poorly understood process that creates an intracellular, membrane-bound channel without any associated cell junctions (Fig. 1D) (Guillemin et al., 1996; Lubarsky and Krasnow, 2003). This process of outgrowth and lumen formation is repeated many times during the 5 days of larval life so that by the end of the third larval instar a single terminal cell has formed dozens of terminal branches, each with a single air-filled lumen, that are neatly matched to the oxygen needs of the target (Fig.

Department of Biochemistry and Howard Hughes Medical Institute, Stanford University School of Medicine, Stanford, CA 94305-5307, USA.

*Author for correspondence (e-mail: krasnow@cmgm.stanford.edu)

1C,D). Although signaling pathways and transcription factors that control branch sprouting and outgrowth have been characterized (Affolter et al., 2003; Ghabrial et al., 2003; Uv et al., 2003; Zelzer and Shilo, 2000), downstream effectors that mediate outgrowth, lumen formation, substrate attachment and branch maintenance remain to be identified.

Here, we describe a complementation group called *tendrils* identified in a genetic mosaic screen for tracheal mutants. *tendrils* mutations cause a dramatic alteration in terminal branch lumen organization and a reduction in terminal branch number. We provide evidence that these phenotypes arise late in development from a defect in branch maintenance. *tendrils* is allelic to *rhea*, the gene that encodes the *Drosophila* talin (Brown et al., 2002), a large cytoskeletal protein that links integrin cell-adhesion molecules to the cytoskeleton (Calderwood and Ginsberg, 2003; Calderwood et al., 1999; Garcia-Alvarez et al., 2003). The major β-integrin of *Drosophila* localizes along the basal surface of terminal branches, and terminal cells lacking this integrin or the α-integrins Multiple edematous wings and Inflated exhibit the *tendrils* phenotype. The results suggest that integrin-talin adhesion complexes anchor mature terminal branches to their substrata and maintain luminal organization. In the absence of these complexes, lumens become disorganized and retract from branches, and lumenless branches degenerate.

MATERIALS AND METHODS

Fly strains
tendrils mutations were induced by ethyl methanesulfonate (EMS) on an FRT^{2A}, FRT^{82B} chromosome and isolated in a screen described elsewhere (A.S.G., B.P.L. and M.A.K., unpublished). A *UAS-GFP* RNAi transgene insertion on chromosome arm 3L (A.S.G., B.P.L. and M.A.K., unpublished) was recombined onto a *ru h th st* FRT^{2A} chromosome. The following mutants have been described (see www.flybase.org and references noted): $rhea^1$, $rhea^2$ and $rhea^{79}$, a deficiency that removes the *rhea* locus and part or all of two flanking genes (Brown et al., 2002; Prout et al., 1997); *myospheroid*^{XG43} (*mys*) (Bunch et al., 1992), mys^{M2} and mys^{G4} (Jannuzi et al., 2002); *inflated*^{k27e} (*if*), *multiple edematous wings*^{M6} (*mew*) and if^{k27e} mew^{M6} double mutant; $scab^1$; and *integrin linked kinase*^{1} (*ilk*), *blistery*$^{3R-13}$ (*by*), *vinculin*^{1} (*vinc*) and *steamer duck*$^{3R-17}$ (*stck*). Mutations that were viable through the third larval instar were analyzed as homozygotes. Others were recombined as necessary onto FRT bearing chromosomes [FRT^{19A}(X), FRT^{40A}(2L), FRT^{G13}(2R), FRT^{2A}(3L) or FRT^{82B}(3R) as appropriate] and analyzed in genetic mosaics. Germline clones of $rhea^{79}$ were generated by the dominant female sterile technique (Chou and Perrimon, 1996). For analysis of maternal-zygotic *tendrils* mutant embryos, $rhea^{79}$ eggs generated this way were fertilized with *tendrils*$^{13-8}$ or *tendrils*$^{6-66}$ sperm.

Mosaic analysis
Embryos harboring $hsFLP^{122}$, *btl-Gal4*, *UAS-GFP* and/or *UAS-DsRed*, and the mutation of interest on an FRT chromosome in trans to a chromosome containing an identical FRT insertion and either *UAS-Gal80* (Lee and Luo, 1999) or GFP RNAi (*UAS-GFPi*; A.S.G., B.P.L. and M.A.K., unpublished) transgenes, were collected 0-4 hours after egg lay (AEL). Embryos were subjected to a 38°C heat shock for 45-60 minutes to induce expression of FLP recombinase, and then allowed to develop at 25°C for the times noted. Homozygous mutant tracheal cell clones lack the dominant repressor (*UAS-Gal80* or *UAS-GFPi*) and express GFP (*btl-Gal4*, *UAS-GFP*). For whole-mount analysis, larvae were mounted in 50% glycerol, killed by heating on a 70°C block for ~5 seconds, and examined with an Axiophot compound fluorescence microscope equipped with a CCD camera.

For quantification of phenotypes, mosaic wandering third instar larvae were analyzed. The number of lumen tips and branch tips in individual terminal cells were counted and used to calculate the lumen:branch ratio. Lumen tip number could be reliably ascertained up to approximately six tips per branch. Only mature branches in which a cytoplasmic process was visible by GFP fluorescence and a lumen was visible under bright-field optics were counted. To quantify branch loss, the number of branch tips in each mutant terminal cell was compared with the number in the contralateral wild-type cell.

Tracking development of mutant clones
Individual terminal cells marked with GFP were identified in early L3 mosaic larvae anesthetized with ether. The mutant cell was imaged as above, and the larva was placed in a fresh vial and allowed to continue development at 25°C. After 48 hours, the larva was heat killed, and the mutant cell was imaged again. Contralateral wild-type terminal cells served as controls.

Genetic mapping
Two rounds of meiotic recombination mapping of *tendrils*$^{13-8}$ were carried out using an isogenized mapping chromosome (*ru h th st cu sr e ca*). Recombinants were tested for complementation of *tendrils*$^{15-39}$. SNP markers have been described (Berger et al., 2001). SNP 3L078A [5′ATCTTGTAACCT(A/C)GGGGGTTGCAC] is an *Avr*II RFLP identified here that was amplified by PCR with primers 5′GCGGACCAAGA-ACCCAGTGACAAC and 5′GTTCCTCGAAGTGACCCGAATGTCC. Complementation tests were carried out between *tendrils*$^{15-39}$ and chromosomal deficiencies *Df(3L)ZP1*, *Df(3L)66C-G28* and *Df(3L) BSC13*, and the mutations $rhea^1$, *cbl*^{KG03080}, *hairy*^{22}, *l(3)DTS4*^{1}, *l(3)L0139*, *l(3)j8E8*, *l(3)neo13* and *Grunge*^{03928}.

DNA sequencing
tendrils alleles were rebalanced over TM3 *Sb twi-Gal4,UAS-GFP* (FlyBase). Homozygous *tendrils* embryos were identified by absence of GFP. DNA was extracted using Chelex beads (Walsh et al., 1991). All *rhea* exons and splice sites were amplified by PCR and sequenced.

Analysis of *tendrils*$^{13-8}$ splicing defect
RNA was isolated with Trizol reagent (Invitrogen) from *tendrils*$^{13-8}$/*rhea*^{79} embryos derived from $rhea^{79}$ germline clones. cDNA was prepared using PowerScript reverse transcriptase (BD Biosciences) and primer 5′CGCTGTGGCTCCGTCAGATTTAC. Talin cDNA was amplified by PCR using primers 5′TTACCCAAGGAAACGACGAC and 5′AAGGTA-ACGCCGTAGGTGG flanking the fourth intron. PCR products were sequenced to determine the splicing pattern.

Immunostaining
L3 larvae were filleted open along the ventral midline, dissected in 3.7% formaldehyde/phosphate-buffered saline (PBS), fixed for 20 minutes at room temperature, then transferred to 100% methanol at –20°C for at least 20 minutes. Samples were rehydrated into PBS with 0.3% Triton X-100 (PBST). Antigen blocking was at room temperature for 30 minutes in PBST with 0.2% BSA (PBSTB). Subsequent incubations were carried out in PBSTB as described (Patel, 1994). Primary antibody incubations were at room temperature for 2 hours or 4°C overnight. Primary antibodies were anti-β$_{mys}$-integrin mAb CF6G11 (Developmental Studies Hybridoma Bank; 1:1000 dilution) and rabbit anti-GFP (Molecular Probes; 1:500). Secondary antibodies coupled to Cy2 and Cy3 (Jackson ImmunoResearch) were used at 1:500. Samples were mounted in ProLong media (Molecular Probes) and images acquired on a BioRad 1024 confocal fluorescence microscope and adjusted using Adobe Photoshop. Embryo fixation and staining was as described (Samakovlis et al., 1996), except maternal-zygotic *tendrils* embryos were stained with a rhodamine-conjugated chitin probe (Devine et al., 2005).

Transmission electron microscopy
Genetic mosaic animals were generated as above, except clones were marked with GFP and CD2-HRP (Larsen et al., 2003; Watts et al., 2004). Mosaic larvae were identified by GFP fluorescence, dissected in PBS, and immediately fixed for 15 minutes at room temperature in 2.5% glutaraldehyde/PBS. Horseradish peroxidase (HRP) signal was enhanced using biotin-labeled tyramide amplification (PerkinElmer) and avidin-HRP, and developed with diaminobenzidine (DAB) and NiCl for 5-10 minutes at room temperature (Vectastain Elite, Vector Laboratories). Clones were photographed, and fillets were postfixed for 1 hour at room temperature in 1% osmium tetraoxide and stained overnight in 0.5% uranyl acetate. After dehydration into 100% ethanol, samples were infiltrated with EMbed 812

resin (Electron Microscopy Sciences) and oriented in casts for sectioning. Sectioning with a Leica UCT microtome and imaging on a Jeol TEM1230 electron microscope were carried out as described (Watts et al., 2004). Images were acquired with a CCD camera and adjusted using Adobe Photoshop. Tracheal clones were identified by electron dense precipitate at the plasma membrane, and their lumens by the ridged cuticle lining.

RESULTS
tendrils terminal cells have multiple, convoluted lumens and few branches

In a genetic mosaic screen designed to saturate the third chromosome for EMS-induced mutations affecting tracheal development (A.S.G., B.P.L. and M.A.K., unpublished), we identified six independent mutations that caused a novel lumen defect in tracheal terminal cell clones. Wild-type third instar larval

terminal cells have over a dozen branches (Fig. 1C,E), each of which contains a single air-filled lumen coursing smoothly along its length (Fig. 1F,I,J). By contrast, terminal cells homozygous for any of the six mutations had multiple and highly convoluted lumens (Fig. 1G). Transmission electron microscopy (TEM) of terminal cell clones demonstrated that multiple lumens were present within single terminal branches (Fig. 1L), as plasma membrane surrounded groups of lumens but was not detected between lumens (Fig. 1M). Mutant terminal branches were typically thicker than in wild type (Fig. 1F,G,I,L). All terminal cells examined were affected, including lateral trunk, ganglionic, visceral and fat body terminal cells (Fig. 1O and data not shown), whereas other types of tracheal cells, including stalk cells, fusion cells and dorsal trunk cells appeared normal (Fig. 1N and data not shown). Complementation tests demonstrated that four of the mutants, 6-66, 13-8, 14-69 and 15-39

Fig. 1. Tracheal luminal phenotype of *tendrils* mutations. (**A**,**B**) Dorsal and lateral views of third instar larval tracheal system (Rühle, 1932). Positions of lateral trunk (LT), dorsal trunk (DT), dorsal branch (DB), fat body branch (FB) and visceral branch (VB) are indicated. Anterior is leftwards. Dorsal is upwards in B. (**C**) Fluorescence micrograph montage of two DBs and their terminal cells (corresponding to boxed region in A) in mosaic third instar larva. Tracheal system is labeled with DsRed; DB terminal cell clone on the right is marked with GFP. Each terminal cell forms over a dozen terminal branches that attach tightly to the underlying muscles. s, DB stalk connecting DB to DT. f, fusion branch formed by individual cell connecting DB to contralateral DB. Arrowhead, DB terminal cell nucleus. Broken line indicates continuation of DB outside focal plane. (**D**) Schematic of terminal cell with multiple terminal branches (cellular projections), each with a membrane-bound lumen coursing through it. (**E**) Wild-type (*tendrils*[+]) DB terminal cell clone induced in 2- to 4-hour-old embryo marked with cytoplasmic GFP and examined in wandering third instar larvae. (**F**) Fluorescent (left; 'cytoplasm'), bright-field (middle; 'lumen') and merged (right) images of boxed region in E. There is a single lumen (GFP-excluded region in left panel, refractile region in middle panel) in the center of each branch. (**G**) Similar view of a homozygous *tendrils*[6-66] DB terminal cell clone. Multiple convoluted lumens of different sizes are present in a single thick branch. (**H-J**) TEM analysis of *tendrils*[+] DB terminal cell clone induced as above and marked with GFP and CD2-HRP. (H) Clone visualized by DAB staining prior to sectioning. Broken line indicates approximate sectioning plane. (I) Section through terminal branch of the clone. An electron dense layer of DAB staining is present at the plasma membrane. A single lumen (red dot) is present in cross section through branch. tc, terminal cell; m, muscle. (J) Higher magnification of the lumen in I. (**K-M**) Similar analysis of a *tendrils*[−] *(rhea*[79]) clone. More than 25 lumen cross-sections are visible in L, all in the same terminal branch (as shown by absence of basal plasma membrane between lumens in M). (**N**) Fluorescence (left) and bright-field (right) images of *tendrils*[13-8] DB clones (marked with GFP) that include one of the two terminal cells shown (arrow) as well as neighboring fusion (f) and stalk (s) cells. Only the mutant terminal cell (arrow) is affected. Mutant stalk and fusion cells, and neighboring *tendrils*[+] terminal cell (arrowhead) are indistinguishable from wild type. (**O**) *tendrils*[13-8] fat body (FB) terminal cell clone as in N. Multiple convoluted lumens are present in single terminal branch, similar to DB terminal cell clones in G and N. Scale bars: 100 μm in C; 25 μm in E; in G, 25 μm for F,G; 25 μm in N,O; in I, 2 μm for I,L; in J, 0.5 μm for J,M.
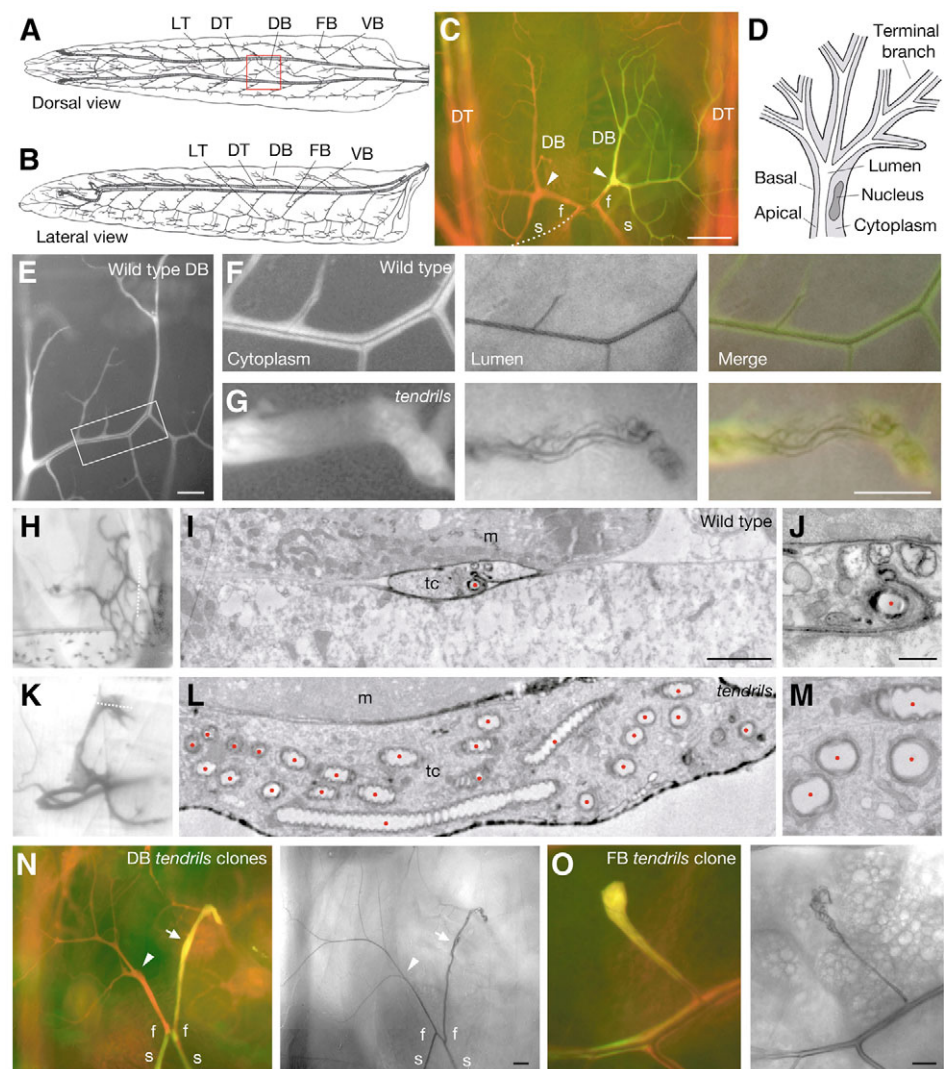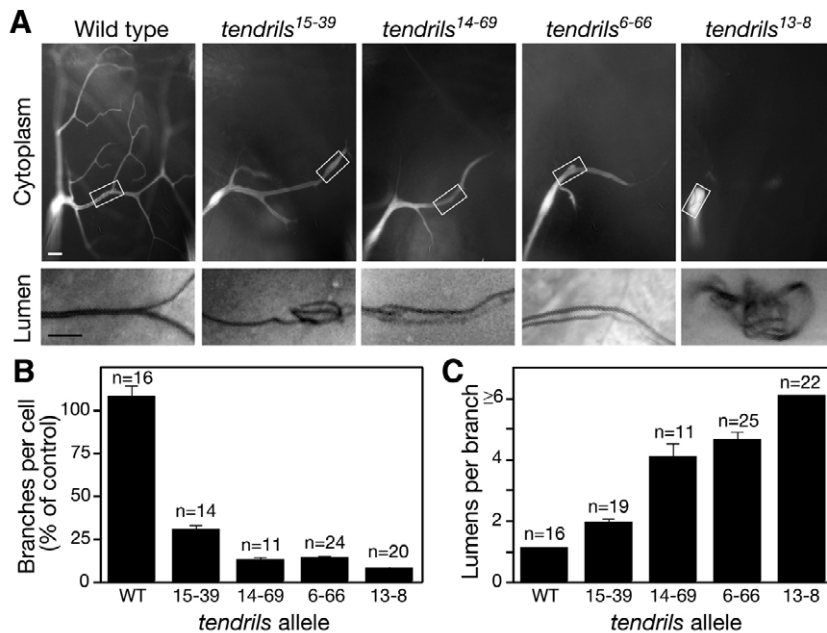
Fig. 2. Effect of *tendrils* mutations on terminal cell branching. (**A**) Fluorescent images of homozygous *tendrils*⁺ and *tendrils*⁻ DB terminal cells clones in sixth tracheal metamere of wandering third instar larvae. White boxes, region enlarged in bright-field image below showing lumen. Scale bars: 20 μm in cytoplasm; 10 μm in lumen. (**B**) Quantification of terminal branching phenotype of *tendrils* alleles. Number of terminal branches in DB terminal cell clone was counted and compared with number in control contralateral *tendrils*⁺ terminal cell. Values shown are mean (±s.e.m.). *n*, number of terminal cells analyzed. (**C**) Quantification of lumen phenotype of *tendrils* alleles. The number of lumens in each clone was counted and divided by the number of terminal branches. Values above six lumens per branch are plotted together because of difficulty in obtaining accurate counts at high lumen density. The severity of terminal branch loss (B) parallels the severity of the lumen phenotype (C) in this series of alleles.

define a lethal complementation group, which we named *tendrils* because mutant terminal cell lumens resembled the convoluted structure of plant tendrils.

The four *tendrils* mutations compose an allelic series with luminal defects of increasing severity: *tendrils*⁺<*tendrils*¹⁵⁻³⁹<*tendrils*¹⁴⁻⁶⁹, *tendrils*⁶⁻⁶⁶<*tendrils*¹³⁻⁸. In the weakest allele, *tendrils*¹⁵⁻³⁹, most branches contained a single, smooth, air-filled lumen as in wild-type branches (Fig. 2A,C). However, in the tips of some branches, the lumen was convoluted or extra lumens were present. In the moderate alleles, *tendrils*¹⁴⁻⁶⁹ and *tendrils*⁶⁻⁶⁶, almost every lumen appeared convoluted and all branches contained multiple lumens. In the strongest allele, *tendrils*¹³⁻⁸, a massive tangle of lumens was packed into a sphere of cytoplasm. When multiple lumens were present within a branch, they were not always the same diameter, a result we explain in the Discussion (Fig. 1G, Fig. 2A).

In addition to the effects on lumen number, organization and size, *tendrils* mutations reduced the number of terminal branches. Dorsal terminal cells in wild-type third instar larvae contained 16±5 mature branches (*n*=32) (Fig. 2A,B). Terminal cell clones homozygous for the weak *tendrils* allele (*tendrils*¹⁵⁻³⁹) had ~70% fewer terminal branches than normal, the moderate alleles (*tendrils*¹⁴⁻⁶⁹, *tendrils*⁶⁻⁶⁶) showed a ~90% reduction in branches and the strongest allele (*tendrils*¹³⁻⁸) displayed an almost complete loss of terminal branches. The severity of terminal branch reduction paralleled the strength of the multi-lumen phenotype (Fig. 2B,C).

Both the multi-lumen and terminal branch reduction defects were strictly cell autonomous. Cells neighboring *tendrils* clones, including other terminal cells, had normal morphology (Fig. 1N). *tendrils* mutations are recessive as terminal cell morphology in *tendrils* heterozygotes was indistinguishable from wild type.

The *tendrils* phenotype arises late in development from failure to maintain branches

The clonal analysis examined the *tendrils* effect on terminal cells at the end of third larval instar, five days after fertilization. We analyzed *tendrils* terminal cells at earlier stages of development to determine when defects arise and how they progress. The first terminal branches sprout late in embryogenesis, ~13-20 hours after fertilization. These sprouts developed normally in homozygous

tendrils embryos, as assessed by staining fixed embryos for a tracheal luminal antigen (2A12) and cytoplasmic marker (*btl-Gal4, UAS-GFP*) (data not shown). This appears to be true also in embryos lacking maternal as well as zygotic *tendrils*, although this was difficult to ascertain rigorously owing to global developmental defects in these embryos.

Because homozygous *tendrils* mutants did not survive beyond embryogenesis, we examined the tracheal phenotype of developing larvae in dorsal branch terminal cell clones of the strong *tendrils*¹³⁻⁸ mutant (Fig. 3A-C). By early second instar, *tendrils*¹³⁻⁸ mutant terminal cell clones had formed multiple terminal branches with normal lumen morphology and appeared grossly similar to neighboring wild-type terminal cells, although in some clones we noticed a slight reduction in the number of terminal branch sprouts (Fig. 3A). In early third instar, defects became prominent in *tendrils*¹³⁻⁸ clones. The number of terminal branches was significantly reduced relative to wild-type terminal cells, and the lumens of the branches in mutant terminal cells were convoluted (Fig. 3B). By late third instar larvae, the phenotype was dramatic. *tendrils*¹³⁻⁸ mutant terminal cells typically had just a single stubby branch packed with a tangle of convoluted lumens (Fig. 3C). Thus, early stages of terminal cell development proceed normally in *tendrils* mutant cells, and defects become prominent during the third instar, several days after terminal branches have begun sprouting and forming air-filled lumens.

Phenotypic progression was also assessed by examining individual terminal cell clones twice during third larval instar. This was carried out by characterizing GFP-labeled clones in live, anesthetized larvae, then placing the larvae in fresh vials and re-examining the same clones 48 hours later. Fig. 3D shows a representative *tendrils*¹³⁻⁸ mutant terminal cell clone in an anesthetized early third instar larva, which appears similar to the clones described above in heat-killed larvae of the same age: there were multiple terminal branches, each containing one or more convoluted lumens. The same mutant cell 48 hours later is shown in Fig. 3E,E′. Terminal branches 1, 2 and 3 have been lost and there is a corresponding increase in number of lumens in the remaining branch. The neighboring control *tendrils*⁺ terminal cell did not show any branch loss or change in lumen morphology during the same
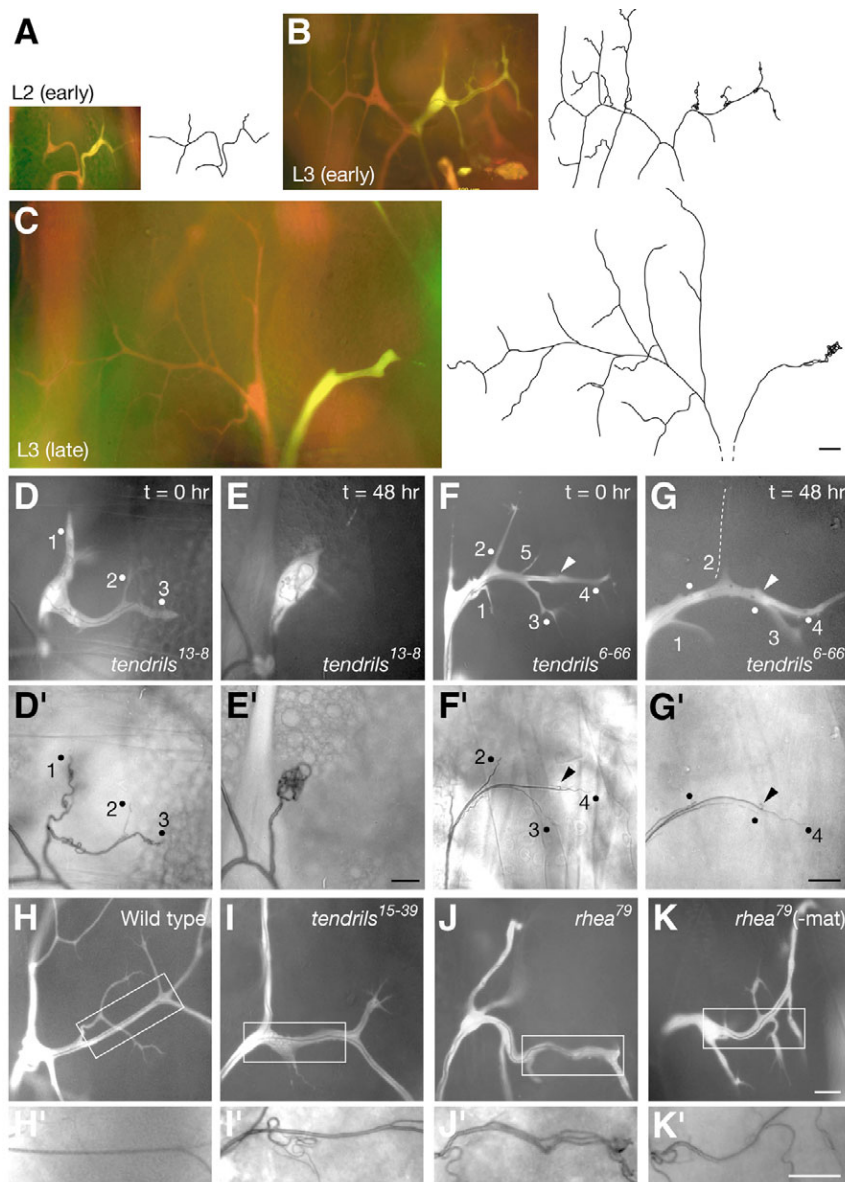
Fig. 3. Onset and progression of *tendrils* phenotype. (**A-C**) *tendrils*[13-8] DB terminal cell clones (yellow) and contralateral *tendrils*[+] control (red) at larval stages indicated. Lumen tracings of corresponding bright-field images are shown at right. At early L2 *tendrils*[13-8] mutant cells resemble *tendrils*^{+} cells, whereas *tendrils*[13-8] clones examined later in development have progressively more severe phenotypes. (**D,E**) *tendrils*[13-8] DB terminal cell clone imaged live in early L3 larva (D, GFP fluorescence; D′, bright-field) and again 48 hours later (E,E′). Numbers indicate specific branches; dots indicate distal end of air-filled lumen. Terminal branches (1, 2, 3) are lost and their lumens compact into soma during a 48-hour period. Contralateral *tendrils*[+] control cell (not shown) continued to develop normally. (**F,G**) Similar analysis of *tendrils*[6-66] DB terminal cell clone. The convoluted lumens of branches 2 and 3 are displaced into the more proximal branch and branch 2 becomes extremely thin (broken line) during 48-hour period. The lumen of branch 4 is also displaced, as monitored by the position of a lumen spur (arrowhead) with respect to branch 3. (**H-K**) Effect of elimination of maternal *tendrils*[+] function on *tendrils* phenotype. Fluorescent images (H-K) and bright-field close-ups (H′-K′) of *tendrils*[+] (H) and *tendrils*[–] (I,J) DB terminal cell clones generated in animals derived from *tendrils*[+] (H-J) or *tendrils*[–] (K) eggs. *tendrils* phenotype (I,I′,J,J′) is not enhanced when maternal *tendrils*[+] is eliminated (K,K′). Scale bars: 25 μm . Bar in C applies to A-C; bar in E′ applies to D,E; bar in G′ applies to F,G; bar in K applies to H-K; bar in K′ applies to H′-K′.
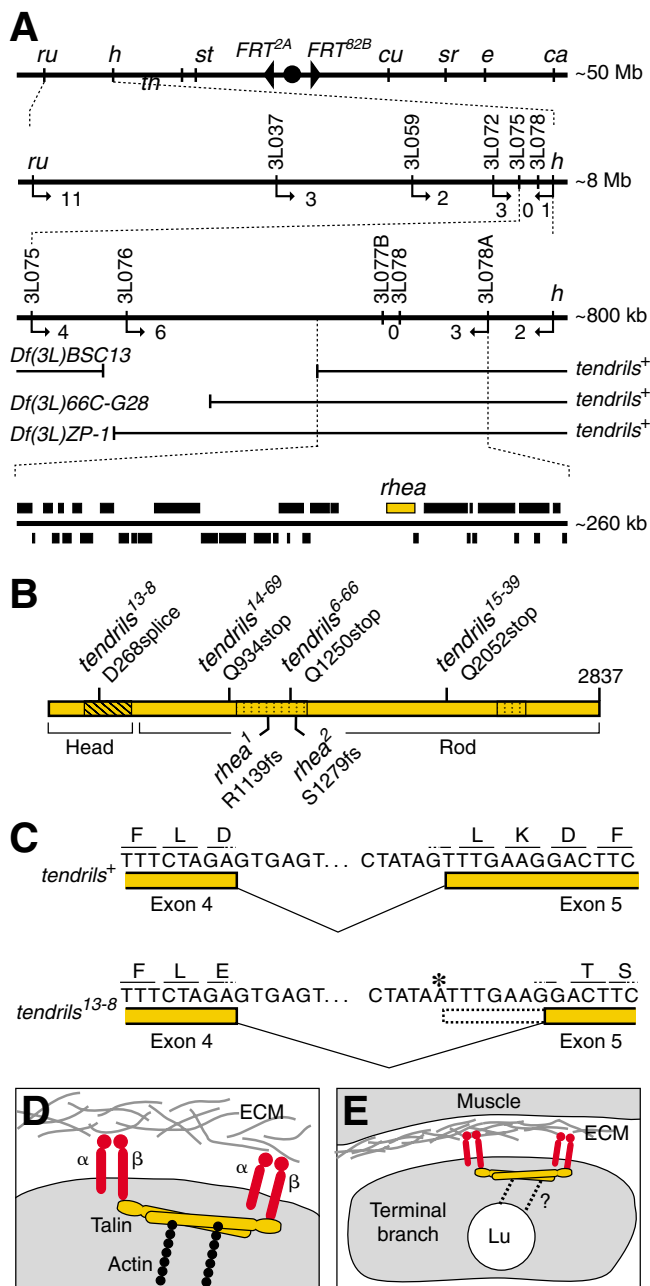
period (data not shown). When the moderate allele *tendrils*[6-66] and the *rhea*[79] allele described below were analyzed in the same way, a similar loss of branches and increase in lumen number in the remaining branches occurred during the 48-hour period, although the effects were less extensive and occasionally no branches were lost during the observation period (Fig. 3F,G; data not shown). In clones of the moderate alleles, we often detected thin terminal branches whose lumen was displaced into the proximal terminal branch during the 48 hour period (e.g. branches 2, 3 in Fig. 3F-G′). These branches lacking lumens are likely to be intermediates in the process of degenerating. Thus, the *tendrils* phenotype appears to result from a catastrophic event(s) late in terminal cell development that disrupts lumen organization, and destabilizes and ultimately destroys terminal branches.

We tested whether the late onset of the *tendrils* phenotype was due to persistence of maternally expressed wild-type *tendrils* gene product. Null *tendrils* mutant terminal cell clones (*rhea*[79]/*rhea*[79], see below) were generated in heterozygous embryos derived from eggs lacking maternal *tendrils* (*rhea*[79] germline clones) fertilized by *tendrils*[+] sperm. These *tendrils* mutant terminal cell clones showed

a phenotype indistinguishable from that of clones of the same genotype generated in embryos with the full maternal *tendrils* contribution (compare Fig. 3J with 3K). Thus, maternal expression does not influence the terminal cell phenotype.

tendrils is allelic to *rhea*, the *Drosophila* talin

To initiate molecular analysis of *tendrils*, we mapped the *tendrils* locus and identified the gene (Fig. 4A). Initial meiotic recombination mapping using visible genetic markers placed *tendrils*[13-8] between *roughoid* and *hairy* on chromosome III. Subsequent high-resolution recombination mapping with SNP markers (Berger et al., 2001) and mapping with chromosomal deficiencies in the region localized *tendrils* to a ~260 kb interval between cytological positions 66D2 and 66D8-9. All known lethal mutations in the candidate interval were tested for their ability to complement *tendrils* mutations for viability. The *tendrils* alleles all failed to complement mutations in *rhea*, the gene encoding *Drosophila* talin (Brown et al., 2002). Terminal cell clones of *rhea*[2] and *rhea*[79] were generated and showed the *tendrils* phenotype, similar in severity to moderate *tendrils* alleles (Fig. 3I-J′; data not shown).

Fig. 4. Mapping and molecular characterization of tendrils mutations. (**A**) Meiotic and deficiency mapping of *tendrils[13-8]*. Initial mapping placed *tendrils[13-8]* between *roughoid* (*ru*) and *hairy* (*h*) on chromosome 3 (top line). Markers used for mapping, FRT sites (triangles) and centromere (closed circle) are indicated. Second line shows *ru-h* interval with SNP markers used for mapping. Number of recombinant breakpoints in each SNP interval (out of 20 *ru-h* recombinants from first round of mapping) is shown below the line; arrows show direction of *tendrils[13-8]* relative to SNP markers. Third line shows *3L075-h* interval along with the combined results of first and second rounds of mapping (235 *ru-h* recombinants). The structure of three deficiency chromosomes and complementation results with *tendrils[13-8]* are shown below the line. Gaps indicate minimal sizes of the deficiencies from published cytology. Fourth line shows genes (black boxes) in region between *Df(3L)BSC13* proximal breakpoint and *3L078A*. *tendrils[13-8]* failed to complement *rhea[1]* (gold box), which encodes talin. (**B**) Changes in talin-coding sequence in *tendrils* alleles. *tendrils[13-8]* alters a 3′ splice site in the fourth intron (see C) that results in mis-splicing, which changes codon D268 and beyond (see panel C). Putative head and rod regions, FERM- and F-actin-binding domain (hatched rectangle), and F-actin-binding domains (stippled rectangles) are indicated (Brown et al., 2002). (**C**) Sequences of fourth intron splice junctions of talin gene in wild-type (*tendrils[+]*) and *tendrils[13-8]* mutant. *tendrils[13-8]* has a G>A mutation (asterisk) in the 3′ splice site that leads to use of a cryptic 3′ splice site seven nucleotides downstream, as determined by RT-PCR analysis of *tendrils[13-8]* RNA. (**D**) Diagram of talin dimer linking cell-surface integrin to actin cytoskeleton. Talin head binds to cytoplasmic domain of β-integrin subunit; rod domain contains actin binding sites. Modified, with permission, from Calderwood and Ginsberg (Calderwood and Ginsberg, 2003). (**E**) Model of talin function in tracheal terminal cells. Talin associates with a β-integrin at the basal surface of the terminal branches and stabilizes binding to the muscle. We speculate that talin also associates with the cytoskeleton and stabilizes lumen (Lu) position in the cell.

that the mutation causes mis-splicing and use of a cryptic 3′ splice site located seven nucleotides 3′ of the normal site. This alters codon 268 and beyond, which truncates talin in the head domain, removing much of the FERM motif and the entire rod domain. We conclude that *tendrils* mutations are alleles of *rhea* and that the *tendrils* alleles constitute a C-terminal deletion series of talin, with the extent of truncation paralleling the severity of the *tendrils* phenotype.

Talin is a large cytoskeletal protein that links the cytoplasmic domain of β-integrins at the plasma membrane to the cytoskeleton (Brown et al., 2002; Calderwood and Ginsberg, 2003) (Fig. 4D). Talins contain an N-terminal head domain with a FERM motif required for binding to β-integrins, actin, PIPKIγ and FAK, and a long C-terminal rod with two higher affinity F-actin binding domains (Fig. 4B) (Brown et al., 2002; Calderwood and Ginsberg, 2003). Sequencing the talin-coding region and RNA splice sites in each *tendrils* mutant identified a single nucleotide change in each allele that alters the coding region or a splice signal (Fig. 4B). *tendrils[14-69]*, *tendrils[6-66]* and *tendrils[15-39]* are nonsense mutations that truncate the coding region after amino acids 933, 1249 and 2051, respectively, eliminating regions of the C-terminal rod domain and one or two F-actin binding domains. The strongest allele, *tendrils[13-8]*, is a G to A substitution in the 3′ splice site of the fourth intron (Fig. 4C). Analysis of *tendrils[13-8]* mRNA by RT-PCR revealed

myospheroid β-integrin and two α-integrins function with talin to maintain terminal branches and luminal organization

Talin is required for integrin-mediated adhesion in *Drosophila* (Brown et al., 2002; Devenport and Brown, 2004), but integrin-independent functions of talins have also been reported (Becam et al., 2005; Borowsky and Hynes, 1998). To determine if talin functions in an integrin-dependent process in terminal cells, we examined the localization and function in terminal cells of βPS [encoded by *myospheroid* (*mys*), hereafter called β_mys-integrin], the major *Drosophila* β-integrin required for virtually all known integrin-mediated processes (Brown et al., 2000; Devenport and Brown, 2004). Localization of β_mys-integrin in third instar larval terminal cells was assessed by immunostaining fillets. β_mys-Integrin was detected in punctae along the periphery of terminal branches (Fig. 5A,A′). These may represent focal adhesions attaching the branches to the underlying tissue.
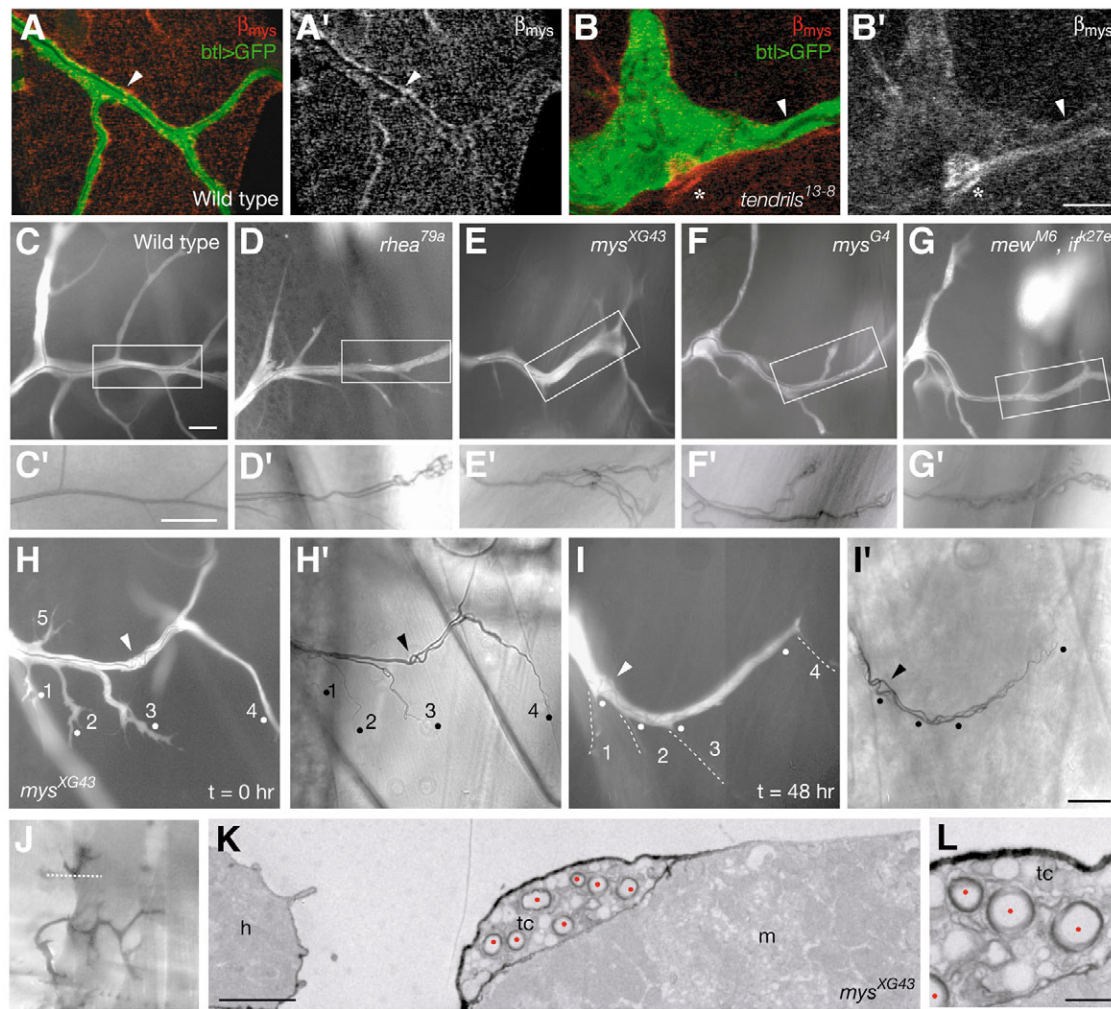
Fig. 5. Tracheal terminal cell expression and mutant phenotype of *myospheroid* integrins. (A-B′) Confocal fluorescent images of *tendrils*+ (A) and *tendrils*[13-8] (B) terminal cell clones in larva fillets stained with mAb CF6G11 to show β_{mys}-integrin (red) and with anti-GFP (green) to show terminal cell cytoplasm. A′ and B′ show β_{mys} staining in gray scale. β_{mys} is found at higher levels in the periphery (arrowhead) of *tendrils*+ but not in *tendrils*[13-8] terminal branches. Terminal branches adhere to muscles that also express β_{mys}. Bright β_{mys} staining in B (asterisk) is outside the tracheal system. **(C-G)** Fluorescent images and brightfield close ups (C′-G′) of wild-type and homozygous DB terminal cell clones of integrin pathway mutations indicated. (C,C′) Wild-type control. (D,D′) *rhea*[79], (E,E′) *mys*[XG43], amorphic β_{mys}-integrin allele. (F,F′) *mys*[G4], point mutation that disrupts ECM-binding by β_{mys} (Jannuzi et al., 2002). (G,G′) *mew*[M6], *if*[k27e] double mutant. *mys* (E,F) and *mew if* (G) phenotypes are similar to *tendrils* phenotype (D). **(H,I)** *mys*[XG43] DB terminal cell clone imaged in early L3 and again 48 hours later as in Fig. 3D-G. Terminal branches are lost and there is an increase in lumen density and complexity in remaining branches, as in *tendrils* mutants. Specific terminal branches are numbered; dots indicate distal extent of lumens. After 48 hours, branch 5 has been lost, branches 1-4 (broken lines) are barely detectable and their lumens (dots and arrowhead) have been displaced into the proximal branch, as in *tendrils* clones (Fig. 3F,G). Lumen displacement is also evident from changes in position of luminal bifurcation (arrowhead) with respect to branches 2 and 3. Panel I is a montage. **(J-L)** TEM analysis of *mys*[XG43] DB terminal cell clone as in Fig. 1H-M. Terminal cell contains multiple lumens (red dots) without any intervening basal plasma membranes, as shown by close-up (L). tc, terminal cell; m, muscle; h, hemocyte. Scale bars: in A, 20 μm for A,B; in C, 25 μm for C-G; in C′ 25 μm for C′-G′; in I, 25 μm for H,I; 2 μm in K; 0.5 μm in L.

To examine β_{mys}-integrin function, *mys* mutant terminal cell clones were generated. We examined molecular null alleles *mys*[XG43] and *mys*[M2], and *mys*[G4], a point mutation that disrupts ligand binding but is expressed and localized similar to wild-type β_{mys}-integrin (Jannuzi et al., 2002). Mutant clones of all three *mys* alleles shared the distinctive *rhea* phenotype (Fig. 5E,F), with substantial branch pruning and multiple convoluted lumens coursing through the remaining terminal branches, similar to the null allele, *rhea*[79] (Fig. 5D). Ultrastructural analysis of *mys*[XG43] mutant terminal cells confirmed that multiple lumens were present within single terminal branches (Fig. 5J-L), like terminal cells that lack talin (Fig. 1K-M).

When individual *mys*[XG43] terminal cells were imaged in live early third instar larvae and again 48 hours later (Fig. 5H,I), terminal branches were lost (branch 5) or collapsed (branches 1-4) as the multi-lumen defect became more prominent, as in terminal cells that lack talin (Fig. 3D-G′). Indeed, as with moderate talin mutants, lumens were often displaced from branches before the branch was completely lost (branches 1-4). We conclude that β_{mys}-integrin is required along with talin to maintain terminal branches and luminal organization in terminal cells. Consistent with this, the punctate peripheral localization of β_{mys}-integrin required talin (Fig. 5B,B′), as in the developing wing (Brown et al., 2002).

Integrins are αβ heterodimers. Five α-integrin genes are present in the *Drosophila* genome (Brown et al., 2000; Hynes and Zhao, 2000). Mutant terminal cell clones were generated for *if*, *mew* and *scb*, the three α-integrin genes for which loss-of-function mutations are available. None of the single mutations caused any detectable defects in terminal cell morphology when homozygous (data not shown). However homozygous *mew^M6*, *if^k27e* double mutant clones exhibited the *tendrils* phenotype (Fig. 5G,G′) demonstrating that these two α-integrins are genetically redundant and function along with β_mys-integrin in terminal cells. Terminal cell clones mutant for the integrin complex genes *ilk*, *by*, *vinc* and *stck* were also examined and showed normal morphology, suggesting that only rudimentary integrin complexes are required for maintenance of terminal branches (data not shown).

DISCUSSION

We identified a complementation group called *tendrils* that reduces the number of branches in tracheal terminal cell clones, and increases the number and alters the morphology of lumens in the remaining branches. The phenotype arises from a defect in branch maintenance. Terminal branches bud from mutant terminal cells and form lumens normally during embryonic and early larval life. Beginning in the second larval instar, lumens become convoluted and then retract into the parental branch, while the lumenless daughter branches are lost. By the end of larval life, the terminal branches that remain have a striking morphology with multiple convoluted lumens in each branch. *tendrils* is allelic to *rhea*, the *Drosophila* talin, a protein that links integrins to the actin cytoskeleton (Brown et al., 2002; Calderwood and Ginsberg, 2003; Liu et al., 2000). β_mys-Integrin localizes in a talin-dependent manner to discrete domains along the basal surface of terminal branches, and terminal cells mutant for *mys* or doubly mutant for *mew* and *if* α-integrins show the same striking phenotype as cells lacking talin.

The results support a model in which integrins and talin form adhesion complexes in terminal cells, and these complexes are required late in larval life to anchor tracheal terminal branches to the underlying substratum and maintain lumen organization within the branches (Fig. 6). In the absence of these complexes, substrate adhesion is compromised, lumen organization is disrupted, lumens retract from the branches and the lumenless branches degenerate. We consider below the implications of these results and this model for the function of integrins and talin in tracheal branch outgrowth, maintenance and lumen organization, and discuss their significance for other tubular networks.

Integrins and talin are required for maintenance of tracheal terminal branches

Drosophila integrins and talin have been implicated in multiple cell adhesion, migration and spreading events (reviewed by Bokel and Brown, 2002; Brown et al., 2000; Brown et al., 2002), including migration of dorsal epidermis, midgut and salivary glands (Bradley et al., 2003; Devenport and Brown, 2004). By contrast, β_mys-integrin and talin were dispensable for the initial sprouting and outgrowth of tracheal terminal branches. It is unlikely that the other *Drosophila* β-integrin, β_v-integrin, functions in terminal branch budding and outgrowth, as it is expressed specifically in the gut (Devenport and Brown, 2004). This suggests that the crucial role of integrins and talin in tracheal terminal cell development is in branch maintenance rather than outgrowth.

A requirement for α-integrins *mew* and *if* in spreading of tracheal visceral branches along the gut during embryonic development has been demonstrated (Boube et al., 2001). This suggests that integrins may also play a role in tracheal branch outgrowth and spreading, at least for this particular branch at this stage of development. Alternatively, the visceral branch phenotype could be an early manifestation of the proposed branch maintenance function of integrins and talin: the gut undergoes substantial morphogenetic movements at this stage that could stress its association with developing visceral terminal branches and cause their detachment. Indeed, embryos lacking maternal and zygotic talin exhibit a similar visceral branch phenotype as *mew* and *if* mutants (B.P.L., unpublished). However, the overall morphology of the visceral branch and its attachment to the gut are not compromised in the presence of *rhea*, *mys* or *mew if* double mutant terminal cell clones, presumably because wild-type terminal cells neighboring the clone are sufficient to anchor the branch to the gut.
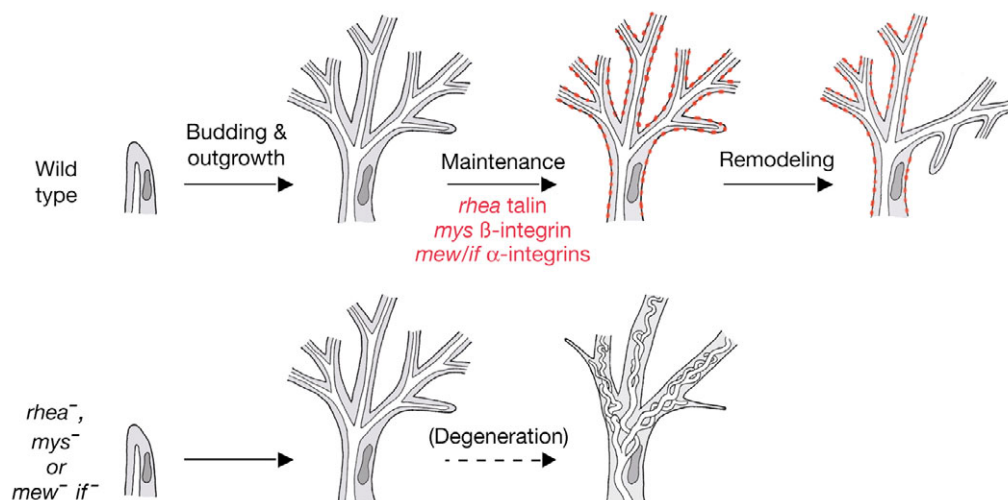

Fig. 6. Model of integrin-talin adhesion complexes in terminal branch maintenance. (Top) Branches sprout from wild-type terminal cells (budding and outgrowth) early in development and are stabilized on their targets (maintenance) by integrin-talin adhesion complexes (red dots). Stabilization may be a reversible process to allow redistribution of branches in response to physiological need (remodeling). (Bottom) Terminal branches sprout normally early in development from *rhea⁻*, *mys⁻* or *mew⁻ if⁻* terminal cells that lack integrin adhesion complexes. However, branches are unstable and their lumens retract into proximal branches as the rest of the branch degenerates (degeneration).

Because integrins and talin are largely dispensable for terminal branch budding and outgrowth, we infer that other cell adhesion system(s) must attach growing terminal branches to their substrata. Indeed, ultrastructural studies reveal 15-20 nm gaps between terminal branches and their substrata, too small to accommodate activated integrins but similar in size to other adhesion junctions including cadherin- and fasciclin-mediated junctions (Noirot and Noirot-Thimotee, 1982; Prokop et al., 1998; Tepass et al., 2000) (B.P.L., unpublished). Interestingly, *tendrils*[13-8] and other mutations that result in C-terminal truncations of talin (Brown et al., 2002) cause a more severe phenotype than deletion of the gene, null *mys* mutations or *mew if* double mutations. This suggests that the remaining N-terminal region of talin has antimorphic effects that interfere with integrin-independent functions of talin, perhaps including its interaction with other cell-adhesion systems. The postulated involvement of two adhesion systems in terminal branch outgrowth could explain why the requirement for β_{mys}-integrin and talin manifests only late in development. Perhaps that is when the outgrowth adhesion system is downregulated and the integrin-talin system becomes necessary to anchor the branches stably to the hypoxic cells they grew out to supply.

Integrins and talin are also required for luminal organization

Surprisingly, the first obvious manifestation of the *tendrils* phenotype in terminal branch development is not loss of branch adhesion but alteration in lumen organization – lumens become convoluted. We also observed lumens of some mutant terminal branches retracting into the parental branch, while the branch it originally occupied was still present and associated with its target. This explains why the residual branches have multiple lumens with different diameters. The results suggest that, in addition to their substrate adhesion function, talin and integrins play an important role maintaining luminal organization within terminal branches. Although the molecular mechanisms of lumen formation and maintenance are unknown, it is likely that the cytoskeleton is crucial for directing assembly of the lumen and maintaining it in a central position within the cytoplasm of each terminal branch (Hogan and Kolodziej, 2002; Lee et al., 2003; Lee and Kolodziej, 2002). Because talin is a crucial mediator of the interaction between integrins and the actin cytoskeleton (Brown et al., 2002; Calderwood and Ginsberg, 2003; Cram and Schwarzbauer, 2004), we speculate that it plays a similar role in tracheal terminal cells and that this interaction is required to support the lumen (Fig. 4D,E). Moesin, a protein that interacts with the microfilament cytoskeleton (Speck et al., 2003), localizes around the lumen in tracheal terminal cells, and this localization is maintained in terminal cells lacking talin (B.P.L., unpublished). This implies that components of the actin cytoskeleton and apicobasal polarity are not grossly disrupted in the mutants, and suggests that talin may play a specific role coupling the apical (luminal) actin network to the basal cell surface, where integrins bind the ECM (Fig. 4E).

A prediction of this model is that mutations in components of the proposed linkage between the ECM and lumen, including other components of integrin-talin adhesion complexes, would also affect lumen organization. None of the mutations we analyzed in other integrin pathway genes had a *tendrils* phenotype, including strong or null mutations in *ilk*, *stck*, *by* and *vinc*. However, another gene identified in our tracheal screen has a *tendrils*-like phenotype, and other complementation groups display defects in lumen organization without affecting branch adhesion or maintenance (A.S.G., B.P.L.

and M.A.K., unpublished). These mutants may help identify additional components of the terminal cell integrin complex and components that link it to the luminal membrane.

Terminal branch degeneration in the absence of integrins and talin

In addition to the striking luminal organization defects observed in *rhea*, *mys* and *mew if* clones, the number of terminal branches was substantially reduced. This reduction results largely from failure to maintain terminal branches, including mature branches complete with air-filled lumens. Absence of integrin-talin complexes in terminal cells thus not only compromises branch adhesion and luminal organization, but also leads to destabilization and destruction of branches. How are destabilized branches eliminated? One possibility is that the branches are degraded, for example, by autophagy or engulfment by phagocytes. Another possibility is that the destabilized branches are subsumed by the parental branch, like cultured fibroblasts that round up when released from their substratum or neuronal processes that retract by a regulated actomyosin-dependent process (Billuart et al., 2001). The retraction mechanism is appealing because it would explain why the remaining branches in mutant terminal cells lacking talin or integrins are thicker than normal – the contents of the daughter branches are consolidated into the parental branch – and why empty basement membranes are sometimes found in positions distal to *tendrils* clones (B.P.L., unpublished).

Although terminal branches normally attach stably to their targets, under hypoxic conditions cellular projections from oxygen-starved cells have been shown to bind nearby terminal branches and redistribute them on the tissue (Wigglesworth, 1959; Wigglesworth, 1977) (E. Johnson and M.A.K., unpublished). Thus, there is a physiological mechanism that can release substrate attachments without leading to branch destruction (Fig. 6, 'remodeling'). It will be interesting to investigate how integrin-talin adhesion complexes are modified during this process and during the much more extensive remodeling of the tracheal network that occurs during metamorphosis.

Branch and lumen maintenance in other tubular networks

Our finding that tracheal terminal branches are actively maintained by an integrin-talin adhesion system raises the issue of whether branches and lumens in other tubular networks also require active maintenance. A parallel is found in aging *C. elegans*, where renal tubules that lose contact with their substratum degenerate in a manner similar to that described here for mutant terminal branches: the distal part of the branch retracts while the lumen is retained as a convoluted tangle in the proximal part of the cell (Buechner, 2002). Disruption of integrin complexes and substrate adhesion in MDCK or endothelial cell in vitro tubulogenesis assays can cause misplacement or absence of lumens (Bayless et al., 2000; Yu et al., 2005), and mutant mice lacking specific integrins or ECM molecules have a variety of tubular defects, some of which might be due to defects in branch or lumen maintenance (McCarty et al., 2002; Wang et al., 2006; Zhu et al., 2002). It will be important to determine the molecular mechanisms of tube maintenance in other systems, and to define the roles that substrate adhesion systems play in maintaining branches and their luminal organization, and destabilizing them during network remodeling events.

References

Affolter, M., Bellusci, S., Itoh, N., Shilo, B., Thiery, J. P. and Werb, Z. (2003). Tube or not tube: remodeling epithelial tissues by branching morphogenesis. *Dev. Cell* **4**, 11-18.

Bayless, K. J., Salazar, R. and Davis, G. E. (2000). RGD-dependent vacuolation and lumen formation observed during endothelial cell morphogenesis in three-dimensional fibrin matrices involves the alpha(v)beta(3) and alpha(5)beta(1) integrins. *Am. J. Pathol.* **156**, 1673-1683.

Becam, I. E., Tanentzapf, G., Lepesant, J. A., Brown, N. H. and Huynh, J. R. (2005). Integrin-independent repression of cadherin transcription by talin during axis formation in Drosophila. *Nat. Cell Biol.* **7**, 510-516.

Berger, J., Suzuki, T., Senti, K. A., Stubbs, J., Schaffner, G. and Dickson, B. J. (2001). Genetic mapping with SNP markers in Drosophila. *Nat. Genet.* **29**, 475-481.

Billuart, P., Winter, C. G., Maresh, A., Zhao, X. and Luo, L. (2001). Regulating axon branch stability: the role of p190 RhoGAP in repressing a retraction signaling pathway. *Cell* **107**, 195-207.

Bokel, C. and Brown, N. H. (2002). Integrins in development: moving on, responding to, and sticking to the extracellular matrix. *Dev. Cell* **3**, 311-321.

Borowsky, M. L. and Hynes, R. O. (1998). Layilin, a novel talin-binding transmembrane protein homologous with C-type lectins, is localized in membrane ruffles. *J. Cell Biol.* **143**, 429-442.

Boube, M., Martin-Bermudo, M. D., Brown, N. H. and Casanova, J. (2001). Specific tracheal migration is mediated by complementary expression of cell surface proteins. *Genes Dev.* **15**, 1554-1562.

Bradley, P. L., Myat, M. M., Comeaux, C. A. and Andrew, D. J. (2003). Posterior migration of the salivary gland requires an intact visceral mesoderm and integrin function. *Dev. Biol.* **257**, 249-262.

Brown, N. H., Gregory, S. L. and Martin-Bermudo, M. D. (2000). Integrins as mediators of morphogenesis in Drosophila. *Dev. Biol.* **223**, 1-16.

Brown, N. H., Gregory, S. L., Rickoll, W. L., Fessler, L. I., Prout, M., White, R. A. and Fristrom, J. W. (2002). Talin is essential for integrin function in Drosophila. *Dev. Cell* **3**, 569-579.

Buechner, M. (2002). Tubes and the single C. elegans excretory cell. *Trends Cell. Biol.* **12**, 479-484.

Bunch, T. A., Salatino, R., Engelsgjerd, M. C., Mukai, L., West, R. F. and Brower, D. L. (1992). Characterization of mutant alleles of myospheroid, the gene encoding the beta subunit of the Drosophila PS integrins. *Genetics* **132**, 519-528.

Calderwood, D. A. and Ginsberg, M. H. (2003). Talin forges the links between integrins and actin. *Nat. Cell Biol.* **5**, 694-697.

Calderwood, D. A., Zent, R., Grant, R., Rees, D. J., Hynes, R. O. and Ginsberg, M. H. (1999). The Talin head domain binds to integrin beta subunit cytoplasmic tails and regulates integrin activation. *J. Biol. Chem.* **274**, 28071-28074.

Chou, T. B. and Perrimon, N. (1996). The autosomal FLP-DFS technique for generating germline mosaics in Drosophila melanogaster. *Genetics* **144**, 1673-1679.

Cram, E. J. and Schwarzbauer, J. E. (2004). The talin wags the dog: new insights into integrin activation. *Trends Cell. Biol.* **14**, 55-57.

Devenport, D. and Brown, N. H. (2004). Morphogenesis in the absence of integrins: mutation of both Drosophila beta subunits prevents midgut migration. *Development* **131**, 5405-5415.

Devine, W. P., Lubarsky, B., Shaw, K., Luschnig, S., Messina, L. and Krasnow, M. A. (2005). Requirement for chitin biosynthesis in epithelial tube morphogenesis. *Proc. Natl. Acad. Sci. USA* **102**, 17014-17019.

Garcia-Alvarez, B., de Pereda, J. M., Calderwood, D. A., Ulmer, T. S., Critchley, D., Campbell, I. D., Ginsberg, M. H. and Liddington, R. C. (2003). Structural determinants of integrin recognition by talin. *Mol. Cell* **11**, 49-58.

Ghabrial, A., Luschnig, S., Metzstein, M. M. and Krasnow, M. A. (2003). Branching morphogenesis of the Drosophila tracheal system. *Annu. Rev. Cell Dev. Biol.* **19**, 623-647.

Green, K. A. and Lund, L. R. (2005). ECM degrading proteases and tissue remodelling in the mammary gland. *BioEssays* **27**, 894-903.

Guillemin, K., Groppe, J., Ducker, K., Treisman, R., Hafen, E., Affolter, M. and Krasnow, M. A. (1996). The pruned gene encodes the Drosophila serum response factor and regulates cytoplasmic outgrowth during terminal branching of the tracheal system. *Development* **122**, 1353-1362.

Hogan, B. L. and Kolodziej, P. A. (2002). Organogenesis: molecular mechanisms of tubulogenesis. *Nat. Rev. Genet.* **3**, 513-523.

Hynes, R. O. and Zhao, Q. (2000). The evolution of cell adhesion. *J. Cell Biol.* **150**, F89-F96.

Inai, T., Mancuso, M., Hashizume, H., Baffert, F., Haskell, A., Baluk, P., Hu-Lowe, D. D., Shalinsky, D. R., Thurston, G., Yancopoulos, G. D. et al. (2004). Inhibition of vascular endothelial growth factor (VEGF) signaling in

cancer causes loss of endothelial fenestrations, regression of tumor vessels, and appearance of basement membrane ghosts. *Am. J. Pathol.* **165**, 35-52.

Jannuzi, A. L., Bunch, T. A., Brabant, M. C., Miller, S. W., Mukai, L., Zavortink, M. and Brower, D. L. (2002). Disruption of C-terminal cytoplasmic domain of betaPS integrin subunit has dominant negative properties in developing Drosophila. *Mol. Biol. Cell* **13**, 1352-1365.

Jarecki, J., Johnson, E. and Krasnow, M. A. (1999). Oxygen regulation of airway branching in Drosophila is mediated by branchless FGF. *Cell* **99**, 211-220.

Larsen, C. W., Hirst, E., Alexandre, C. and Vincent, J. P. (2003). Segment boundary formation in Drosophila embryos. *Development* **130**, 5625-5635.

Lee, M., Lee, S., Zadeh, A. D. and Kolodziej, P. A. (2003). Distinct sites in E-cadherin regulate different steps in Drosophila tracheal tube fusion. *Development* **130**, 5989-5999.

Lee, S. and Kolodziej, P. A. (2002). The plakin Short Stop and the RhoA GTPase are required for E-cadherin-dependent apical surface remodeling during tracheal tube fusion. *Development* **129**, 1509-1520.

Lee, T. and Luo, L. (1999). Mosaic analysis with a repressible cell marker for studies of gene function in neuronal morphogenesis. *Neuron* **22**, 451-461.

Liu, S., Calderwood, D. A. and Ginsberg, M. H. (2000). Integrin cytoplasmic domain-binding proteins. *J. Cell Sci.* **113**, 3563-3571.

Lubarsky, B. and Krasnow, M. A. (2003). Tube morphogenesis: making and shaping biological tubes. *Cell* **112**, 19-28.

Manning, G. and Krasnow, M. (1993). Development of the Drosophila tracheal system. In *The Development of Drosophila melanogaster*. Vol. 1 (ed. M. Bate and A. Martinez-Arias), pp. 609-686. Cold Spring Harbor: Cold Spring Harbor Laboratory Press.

McCarty, J. H., Monahan-Earley, R. A., Brown, L. F., Keller, M., Gerhardt, H., Rubin, K., Shani, M., Dvorak, H. F., Wolburg, H., Bader, B. L. et al. (2002). Defective associations between blood vessels and brain parenchyma lead to cerebral hemorrhage in mice lacking alphav integrins. *Mol. Cell. Biol.* **22**, 7667-7677.

Noirot, C. and Noirot-Thimotee, C. (1982). The structure and development of the tracheal system. In *Insect Ultrastructure*. Vol. 1 (ed. R. C. King and H. Akai), pp. 351-381. New York: Plenum Press.

O'Brien, L. E., Zegers, M. M. and Mostov, K. E. (2002). Building epithelial architecture: insights from three-dimensional culture models. *Nat. Rev. Mol. Cell Biol.* **3**, 531-537.

Patel, N. (1994). Imaging neuronal subsets and other cell types in whole mount Drosophila embryos and larvae using antibody probes. In *Methods in Cell Biology, Drosophila melanogaster: Practical Uses in Cell Biology* (ed. L. S. B. Goldstein and E.A. Fyrberg), Vol. 44, pp. 416-487. New York: Oxford University Press.

Prokop, A., Martin-Bermudo, M. D., Bate, M. and Brown, N. H. (1998). Absence of PS integrins or laminin A affects extracellular adhesion, but not intracellular assembly, of hemiadherens and neuromuscular junctions in Drosophila embryos. *Dev. Biol.* **196**, 58-76.

Prout, M., Damania, Z., Soong, J., Fristrom, D. and Fristrom, J. W. (1997). Autosomal mutations affecting adhesion between wing surfaces in Drosophila melanogaster. *Genetics* **146**, 275-285.

Risau, W. and Flamme, I. (1995). Vasculogenesis. *Annu. Rev. Cell Dev. Biol.* **11**, 73-91.

Rühle, H. (1932). Das larvale tracheensystem von *Drosophila melanogaster* Meigen und seine variabilität. *Z. Wiss. Zool.* **141**, 159-245.

Samakovlis, C., Hacohen, N., Manning, G., Sutherland, D. C., Guillemin, K. and Krasnow, M. A. (1996). Development of the Drosophila tracheal system occurs by a series of morphologically distinct but genetically coupled branching events. *Development* **122**, 1395-1407.

Speck, O., Hughes, S. C., Noren, N. K., Kulikauskas, R. M. and Fehon, R. G. (2003). Moesin functions antagonistically to the Rho pathway to maintain epithelial integrity. *Nature* **421**, 83-87.

Sutherland, D., Samakovlis, C. and Krasnow, M. A. (1996). branchless encodes a Drosophila FGF homolog that controls tracheal cell migration and the pattern of branching. *Cell* **87**, 1091-1101.

Tepass, U., Truong, K., Godt, D., Ikura, M. and Peifer, M. (2000). Cadherins in embryonic and neural morphogenesis. *Nat. Rev. Mol. Cell Biol.* **1**, 91-100.

Uv, A., Cantera, R. and Samakovlis, C. (2003). Drosophila tracheal morphogenesis: intricate cellular solutions to basic plumbing problems. *Trends Cell Biol.* **13**, 301-309.

Walsh, P. S., Metzger, D. A. and Higuchi, R. (1991). Chelex 100 as a medium for simple extraction of DNA for PCR-based typing from forensic material. *Biotechniques* **10**, 506-513.

Wang, J., Hoshijima, M., Lam, J., Zhou, Z., Jokiel, A., Dalton, N. D., Hultenby, K., Ruiz-Lozano, P., Ross, J., Jr, Tryggvason, K. et al. (2006). Cardiomyopathy associated with microcirculation dysfunction in laminin alpha4 chain-deficient mice. *J. Biol. Chem.* **281**, 213-220.

Watts, R. J., Schuldiner, O., Perrino, J., Larsen, C. and Luo, L. (2004). Glia engulf degenerating axons during developmental axon pruning. *Curr. Biol.* **14**, 678-684.

Whitten, J. (1957). The post-embryonic development of the tracheal system in *Drosophila melanogaster*. *Q. J. Microsc. Sci.* **98**, 123-150.

Wigglesworth, V. B. (1959). The role of epidermal cells in the migration of tracheoles in Rhodnius prolixus (Hemiptera). *J. Exp. Biol.* **36**, 632-640.

Wigglesworth, V. B. (1972). *The Principles of Insect Physiology*. London: Chapman & Hall.

Wigglesworth, V. B. (1977). Structural changes in the epidermal cells of Rhodnius during tracheole capture. *J. Cell Sci.* **26**, 161-174.

Wigglesworth, V. B. and Lee, W. M. (1982). The supply of oxygen to the flight muscles of insects: a theory of tracheole physiology. *Tissue Cell* **14**, 501-518.

Yu, W., Datta, A., Leroy, P., O'Brien, L. E., Mak, G., Jou, T. S., Matlin, K. S., Mostov, K. E. and Zegers, M. M. (2005). β1-integrin orients epithelial polarity via rac1 and laminin. *Mol. Biol. Cell* **16**, 433-445.

Zelzer, E. and Shilo, B. Z. (2000). Cell fate choices in Drosophila tracheal morphogenesis. *BioEssays* **22**, 219-226.

Zhu, J., Motejlek, K., Wang, D., Zang, K., Schmidt, A. and Reichardt, L. F. (2002). beta8 integrins are required for vascular morphogenesis in mouse embryos. *Development* **129**, 2891-2903.